Assessment of VMS-LES and hybrid RANS VMS-LES models

A. Belme[1], S. Wornom[2], A. Dervieux[1], B. Koobus[3], M.V. Salvetti[4]

[1]*INRIA, 2004 Route des Lucioles, Sophia-Antipolis, France*
E-mail: Anca.Belme@inria.fr, Alain.Dervieux@inria.fr

[2]*LEMMA, 2000 Route des Lucioles, Sophia-Antipolis, France*
E-mail: Stephen.Wornom@inria.fr

[3] *Dép. Mathématiques, Université de Montpellier, Place E. Bataillon, Montpellier, France*
E-mail: koobus@math.univ-montp2.fr

[4]*Dip. Ingegneria Aerospaziale, Università di Pisa, Via G. Caruso 8, Pisa, Italy*
E-mail: mv.salvetti@dia.unipi.it

Keywords: Turbulence, Large Eddy Simulation, Variational Multiscale, bluff body.

SUMMARY. Turbulent flows around bluff bodies at sub- and supercritical Reynolds numbers are simulated through a Variational Multiscale (VMS) Large Eddy Simulation (LES) model and a hybrid RANS/VMS-LES model. In VMS-LES, the separation between the largest and the smallest resolved scales is obtained through a variational projection operator and finite-volume cell agglomeration. Eddy-viscosity models are used to account for the effects of the unresolved scales. In the VMS approach, they are only added to the smallest resolved ones. We use a hybrid RANS/LES approach with a wall law for the simulation of supercritical turbulent flows. A smooth blending function allows a progressive switch from LES to RANS to be obtained, depending on the values of a blending parameter. The assessment proposed relies on the simulation of a series of flows for which experiments are available. They involve subcritical flows around a circular cylinder at Reynolds numbers (Re) 3900, 10000, 20000, and around a sphere at Reynolds numbers 10000, 50000, and supercritical flows around a circular cylinder (Re=140000, 500000, 1 million, 2 million) and a sphere (Re=400000).

1 INTRODUCTION

Large-Eddy Simulation (LES) is becoming an increasingly popular approach also for applications of industrial or engineering interest, characterized by complex geometries and large Reynolds numbers. Although requiring larger computational resources, LES has the potential to give more accurate results than the Reynolds-Averaged Navier-Stokes (RANS) approach for flows characterized by massive separation or significant unsteadiness. Paradigmatic examples of such flows are bluff-body wakes.

The role and interaction of closure modeling and numerical discretization (grid resolution and schemes) in LES is much different than in RANS and, thus, for application of LES in an industrial context, peculiar issues arise and ad-hoc methodologies and strategies need to be developed and validated. The strategy developed in our previous works [1, 2, 3] is based on the following key ingredients: (i) unstructured grids, (ii) a second-order accurate numerical scheme stabilized by a numerical viscosity proportional to high-order space derivatives, and thus acting on a narrow band of smallest resolved scales, and tuned by an ad-hoc parameter, (iii) Variational MultiScale (VMS) formulation combined with eddy-viscosity subgrid scale (SGS) models. We recall that a key feature of VMS-LES [4] is that the SGS model is only added to the smallest resolved scales. This is aimed at reducing the excessive dissipation introduced by non-dynamic eddy-viscosity SGS models also on the large scales and this has been shown to generally improve the behavior of such models, such as for instance for the Smagorinsky model in boundary layers [5]. This paper concentrates on the use of VMS-LES as LES component, either in pure LES formulation or in hybrid ones.

Indeed, a bottle-neck for LES of high-Reynolds wall-bounded flows is that practical applications carried out now for more than two decades have highlighted that an extremely fine grid resolution, almost comparable to the one of direct numerical simulations, is needed in boundary-layers to obtain accurate results. Clearly, this leads to dramatic computational requirements for large Reynolds numbers. In this context, hybrid strategies have been proposed in the literature, which combine RANS and LES approaches together (see [6, 7] for a review). We developed a hybrid model blending RANS and VMS-LES [8]. In this model, VMS-LES and RANS approaches are combined in such a manner that complexity in use and in parameter tuning is minimized. The closure terms provided by a RANS and a SGS eddy-viscosity model are blended together through the introduction of a blending function which depends on a parameter aimed at identifying whether the used grid is adequate to LES, i.e. if it is adequate to resolve additional fluctuations with respect to RANS. We avoid to use the wall distance in the definition of the blending function, since this yields practical difficulties for complex geometries and complex grid topologies, as e.g. for unstructured grids, especially when parallel computations are carried out. The investigated blending does not require any particular RANS or LES closure and permits a natural integration of the VMS concept.

The benchmarking of our VMS-LES and hybrid RANS/VMS-LES strategies for the flow around a circular cylinder and a sphere is presented herein. Both the subcritical and supercritical regimes are considered, which are respectively characterized by a laminar and a turbulent boundary layer prior separation and correspond to increasingly large Reynolds number. The grid resolution is kept rather coarse, in the perspective of the simulation of complex geometries in an industrial context. The predictions of bulk quantities of engineering interest provided by VMS-LES for subcritical cases and hybrid RANS/VMS-LES for supercritical cases are shown and compared to experimental and numerical data available in the literature. This provides a difficult benchmark for a numerical model, since an adequate description of the boundary layer and of the wake dynamics is needed to obtain accurate predictions of the bulk quantities.

2 METHODOLOGY

The governing equations are discretized in space using a mixed finite-volume/finite-element method applied to unstructured tetrahedrizations. This scheme is a variational one relying on a finite-volume formulation for the convective terms, with a basis and test function χ_l, associated with the finite-volume cell centered on vertex l. A finite-element formulation is used for the diffusive term, with a basis and test function ϕ_l continuous, linear by element, equal to 1 at vertex l and vanishing at other vertexes. The Roe scheme [9] represents the basic upwind component for the numerical evaluation of the convective fluxes. A Turkel-type preconditioning term is introduced to avoid accuracy problems at low Mach numbers [10]. To obtain second-order accuracy in space, the Monotone Upwind Scheme for Conservation Laws reconstruction method (MUSCL) is used, in which the Roe flux is expressed as a function of reconstructed values of W at each side of the interface between two cells. The introduced numerical dissipation is made of sixth-order space derivatives [2] and, thus, concentrates on a narrow-band of the highest resolved frequencies. Finally, an implicit linearized time-marching algorithm is used, based on a backward-difference scheme for the discretization of the time derivative. The numerical method is second-order accurate in space and time. More details can be found in [2].

As far the closure of the RANS equations is concerned, we use the Low Reynolds $k-\varepsilon$ model proposed in [11], which was designed to improve the predictions of the standard $k-\varepsilon$ one for adverse pressure gradient flows, including separated flows. In this model, the Reynolds stress tensor τ^R has the same form as in the standard $k-\varepsilon$ model but the turbulent eddy viscosity is defined by $\mu_t = C_\mu f_\mu \dfrac{k^2}{\varepsilon}$ where $C_\mu = 0.09$ and the damping function f_μ is given by $f_\mu = \dfrac{1-e^{-0.01R_t}}{1-e^{-\sqrt{R_t}}} \max\left[1, \dfrac{\sqrt{2}}{\sqrt{R_t}}\right]$ with $R_t = \frac{k^2}{\nu\varepsilon}$; k and ε are determined by ad-hoc modeled transport equations. In order to master mesh requirements, a wall law is applied in the close vicinity of the wall. We choose the Reichardt analytical law [12] which gives a smooth matching between linear, buffer and logarithmic regions. Because the y^+ normalized distance is generally subject to large variations in complex geometries, we have found mandatory to combine both wall law and low Reynolds modeling which locally damps the fully-turbulent model.

For the LES mode, we consider the VMS approach, in which the resolved flow variables are decomposed as $W = \overline{W} + W'$, where $\overline{W}$ are the large resolved scales (LRS) and W' are the small resolved scales (SRS). We follow here the VMS approach proposed in [13] for the simulation of compressible turbulent flows through a finite volume/finite element discretization on unstructured tetrahedral grids. In order to obtain the VMS flow decomposition, basis and test functions can be expressed as: $\chi_l = \overline{\chi}_l + \chi_l'$ and $\phi_l = \overline{\phi}_l + \phi_l'$, in which the overbar denotes the basis functions spanning the finite dimensional spaces of the large resolved scales and the prime those spanning the SRS spaces. As in [13], the basis functions of the LRS space are defined through a projector operator in the LRS space, based on spatial average on macro cells, which are obtained by an agglomeration process. Eddy-viscosity models are used here for the SGS terms, and more precisely those proposed by Smagorinsky [14] and the so-called WALE model [15]. The eddy-viscosity introduced by these models, within the VMS approach, is computed as a function of the SRS flow variables (small-small approach). Moreover, the key feature of the VMS approach is that the SGS model is added only to the smallest resolved scales. Finally, the SGS terms are discretized analogously to the viscous fluxes. Thus, the Galerkin projection of the LES closure term is: $-\left(\tau^L(W'), \phi_l'\right)$. The filter width Δ involved in the definition of the eddy-viscosity has been set equal to the cubic root of the volume of each tetrahedron. The SGS model constant has been set equal to 0.1 for the Smagorinsky model and to 0.5 for the WALE one.

As previously mentioned, in the hybrid model the RANS and LES closures are blended together; the discretized governing equations are thus the following:

$$\begin{aligned}&\left(\frac{\partial W}{\partial t}, \chi_l\right) + (\nabla \cdot F_c(W), \chi_l) + (\nabla \cdot F_v(W), \phi_l) = \\ &-\theta\left(\tau^R(\langle W\rangle), \phi_l\right) - (1-\theta)\left(\tau^L(W'), \phi_l'\right) \quad l = 1, N\,.\end{aligned} \tag{1}$$

in which $(\cdot,\cdot)$ denotes the L^2 scalar product and F_c and F_v are the convective and viscous fluxes. In Eq. (1), $\langle W\rangle$ should be the RANS mean. In this study, we simply use $\tau^R(W)$, relying on the tendency of RANS to naturally damp the fluctuations. More sophisticated options are possible and will be discussed in forthcoming papers.

At the SRS level, switch from LES to RANS changes the turbulent viscosity model and is not very smooth. At the LRS level, this switch passes from a zero viscosity to ν_{RANS}, a discontinuous switch, except if a progressive blending is installed. As blending function θ, we use $\theta = tanh(\xi^2)$, where ξ is the *blending parameter*, which should indicate whether the grid resolution is fine enough to resolve a significant part of the turbulence fluctuations, i.e. to obtain a LES-like simulation. The choice of the *blending parameter* is clearly a key point for the definition of the present hybrid model. Different options can be used, namely: the ratio between the eddy viscosities given by the LES and the RANS closures, $\xi_{VR} = \mu_s/\mu_t$, the ratio between the LES filter width and a typical length in the RANS approach, $\xi_{LR} = \Delta/l_{RANS}$ with $l_{RANS} = k^{3/2}\epsilon^{-1}$, and, finally, the ratio between characteristic times of the LES and RANS approaches, $\xi_{TR} = t_{LES}/t_{RANS}$ with $t_{LES} = (S_{ij}S_{ij})^{-1/2}$ and $t_{RANS} = k\epsilon^{-1}$. Previous studies [8] indicated that the sensitivity of the results to the choice of the blending parameter is very low.

For the simulations of subcritical flows in the following, only the VMS-LES model is applied, *i.e.* θ is prescribed to be zero and a no-slip wall condition is set.

3 SUBCRITICAL FLOW PAST A CYLINDER

We first investigate the Reynolds number effects for the simulation of the flow past a circular cylinder when the VMS-LES approach is used. A particular Reynolds number interval [3900-20 000] corresponding to the subcritical regime is considered [17] in this analysis. The Reynolds number is based on the cylinder diameter D, and the freestream velocity. The WALE subgrid scale model is used to account for the effect of the unresolved scales. The computational domain is such that $-10 \le x/D \le 25$, $-20 \le y/D \le 20$ and $-\pi/2 \le z/D \le \pi/2$, where x, y and z denote the streamwise, transverse and spanwise directions respectively, the cylinder center being located at $x = y = 0$. No-slip conditions are applied on the cylinder surface. In the spanwise direction, periodic boundary conditions are imposed, while characteristic based conditions are used at the inflow and outflow as well as on the lateral boundaries ($y/D = \pm 20$). The freestream Mach number is set equal to 0.1 in order to make a sensible comparison with incompressible simulations in the literature. Preconditioning is used to deal with the low Mach number regime [3]. For $Re = 3900$, two different grids having 2.9×10^5 and 1.8×10^6 nodes are used. A unique mesh of 1.8×10^6 cells is used for $Re = 10000$ and $Re = 20000$. For all the simulations, statistics are computed by averaging in time over at least 30 vortex shedding cycles, after the initial transient of the solution.

Table 1: Bulk flow parameters at Re=3900. $\overline{C_d}$ is the mean drag coefficient, C_{Lrms} is the r.m.s. of the time variation of the lift coefficient, l_r is the mean bubble recirculation length, $\overline{Cp_b}$ is the value of the mean pressure coefficient in the rear part of the cylinder, θ_{sep} the mean separation angle, and St the Strouhal number.

Simulation	$\overline{C_d}$	C_{Lrms}	l_r	-$\overline{Cp_b}$	θ_{sep}	St
Present VMS-LES	0.99	0.108	1.45	0.88	89	.21
VMS-LES [3] (coarser grid)	1.03	0.377	0.94	1.01	–	.22
VMS-LES [3] (finer grid)	0.94	0.092	1.56	0.83	–	.22
LES [18, 19, 20]	[0.99-1.38]	–	[1.0-1.56]	[0.89-1.23]	–	[0.19-0.21]
Experiments [21, 22, 18, 19]	[0.94-1.04]	–	[1.47-1.51]	[0.82-0.93]	–	[0.20-0.22]

In Tabs.1,2,3 a comparison of our computations with available simulations and experiments is proposed. A general good agreement with the available experimental and numerical data in the literature is observed.

In particular, the Strouhal number associated to vortex shedding slightly decreases as the Reynolds number increases in the considered interval, while the r.m.s. of the lift coefficient increases, as observed for example in [24]. Fig.1 shows that this feature is correctly reproduced in the present VMS-LES simulations. Another important feature observed in the literature is that the formation length of the Karman vortices decreases as the Reynolds number increases. This is shown in Tabs.1,2,3 by the decrease of the mean recirculation bubble length with increasing Reynolds number. This is related with the increase of r.m.s. of the time fluctuations of the lift coefficient. This feature is also well captured in our VMS-LES simulations (see Fig.1b).

Furthermore, in the Achenbach drag-vs-Reynolds curve [16], the interval [3900-20000] corresponds to a section of slow but continuous increment of drag. The drag is reaching a minimum around Re=2000-3000 and increases slowly to a quasi-plateau attained around Reynolds 20000. This feature is also observed in Tabs.1,2,3.

Table 2: Bulk flow parameters at Re=10000. The meaning of the symbols is the same as in Tab. 1.

Simulation	$\overline{C_d}$	C_{Lrms}	l_r	-$\overline{Cp_b}$	θ_{sep}	St
VMS-LES WALE	1.22	0.476	0.87	1.15	87	0.20
DNS [21]	[1.11-1.21]	[0.45-0.57]	0.82	[1.06-1.20]	–	[0.19-0.21]
Experiments [21, 23, 24, 25, 26]	1.19	[0.38-0.53]	0.78	1.11	–	[0.19-0.20]

Table 3: Bulk flow parameters at Re=20000. The meaning of the symbols is the same as in Tab. 1.

Simulation	$\overline{C_d}$	C_{Lrms}	l_r	-$\overline{Cp_b}$	θ_{sep}	St
VMS-LES WALE	1.27	0.60	0.80	1.09	86	0.19
LES [27]	–	–	1.	[1.04-1.25]	–	–
LES [28]	[0.94-1.28]	[0.17-0.65]	[0.7-1.4]	[0.83-1.38]	–	–
Experiments [24, 29, 30, 31]	[1.10-1.20]	[0.4-0.6]	–	[1.03-1.09]	–	0.194

4 SUPERCRITICAL FLOW PAST A CYLINDER

As previously mentioned, the hybrid RANS/VMS-LES approach is used for the simulations of supercritical flow around a circular cylinder. For these simulations, the computational domain is such that $-5 \le x/D \le 15$, $-14 \le y/D \le 14$ and $-1 \le z/D \le 1$, where x, y and z denote the streamwise, transverse and spanwise directions respectively, the cylinder center being located at $x = y = 0$. The boundary conditions and the free-stream Mach number are the same as in the VMS-LES in Sec. 3. The Smagorinsky model is used to close the equations for the VMS-LES part and the hybridization criterion is based on the ratio between characteristic lengths (see Sec. 2).

This study is made of two set of calculations. First, we reproduce a case computed by Travin *et al.* [32] with the DES model, which is at present the most widely used and validated hybrid RANS/LES approach. This $Re = 140000$ flow is made supercritical through the use of RANS close to the wall. Two meshes, with respectively 4.6×10^5 nodes for grid GR1, and 1.4×10^6 nodes for grid GR2 are

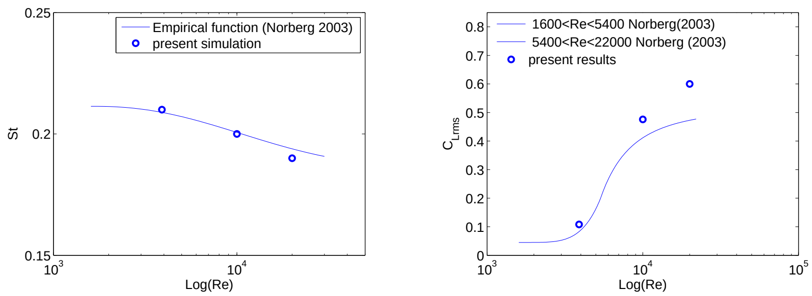

(a) (b)

Figure 1: Comparison of the present results with the empirical functions proposed in [24]; (a) Strouhal number; (b) r.m.s. of the lift coefficient.

used. The main bulk quantities are reported in Table 4 and show a reasonable agreement with the DES outputs.

Table 4: Cylinder, Rey=140 000 (forced supercritical).

Simulation	Re	$\overline{C_d}$	C_l'	St	l_r	$-C_{pb}$
GR1	1.4 10^5	0.62	0.083	0.30	1.19	0.68
GR2	1.4 10^5	0.54	0.065	0.33	1.13	0.63
DES [32]	1.4 10^5	0.57-0.65	0.06-0.1	0.28-0.31	1.1 -1.4	0.65-0.7
DES [33]	1.4 10^5	0.6-0.81	–	0.29-0.3	0.6-0.81	0.85-0.91

The second set of hybrid simulations is carried out at higher Reynolds numbers, viz. Re=500000, 1 million, 2 million, in the supercritical regime. The WALE model is used to close the equations for the VMS-LES part and the hybridization criterion is based on the ratio between the characteristic lengths of LES and RANS. The main bulk parameters obtained in these simulations are reported in Tab. 5, and are compared with experimental and LES data in the literature. A good agreement is observed, especially if we consider the coarse resolution of the employed grids.

5 SUB/SUPERCRITICAL FLOW PAST A SPHERE

As a contribution to the validation of the VMS-LES model alone, we computed the subcritical flows around a sphere at Reynolds numbers 10000 and 50000. The computational domain is such that $-7.5D \leq x \leq 25D$, $-8D \leq y \leq 8D$, and $-8D \leq z \leq 8D$ where D is the sphere diameter. For subcritical cases, a no-slip condition is applied at wall, and a wall law is used for the supercritical case. The corresponding drag values are indicated on Fig.2. The numerical results agree very well with the experimental curve [38]. In the case of Re=50000, vertical wake cuts of the horizontal velocity are compared in Fig.3 with the experiments of Bakic, [39], with a very good accuracy close to the sphere. Some discrepancies are observed more downstream, where the lack of mesh resolution is yet a penalty.

As for the circular cylinder case, we use the hybrid formulation for computing the supercritical

Table 5: Cylinder (Re=$.5 \times 10^6 - 2. \times 10^6$). Main bulk flow quantities. $\overline{C_d}$ is the mean drag coefficient,C_{pb} the value of the mean base pressure coefficient, St the vortex-shedding Strouhal number and l_r the mean recirculation bubble length.

Case		$\overline{C_d}$	$-C_{pb}$	St	l_r
Re=500K	Present,750Kcells	0.22	0.29	0.43	1.50
Re=500K	LES[34]	0.33	–	–	–
Re=500K	Exp.[35]	0.22	0.27	0.45	–
Re=1M	Present,750Kcells	0.27	0.34	0.44	1.42
Re=1M	LES[34]	0.31	0.32	0.35	1.04
Re=1M	Exp.[37, 35]	0.3	0.4	0.45	–
Re=2M	Present,750Kcells	.37	.34	.30	1.87
Re=2M	LES[34]	.32	–	–	–
Re=2M	Exp.[35]	.37	–	.4	–

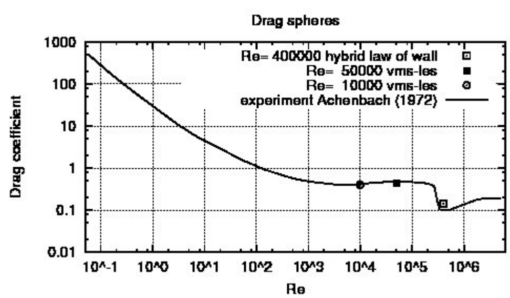

Figure 2: Flow past a sphere: Study of computed drag as a function of Reynolds number. Experiments from Achenbach [38]

flow at a Reynolds number of 400000 with a mesh of 500000 nodes. Fig.2 shows that the prediction of drag is in good agreement with experimental data also for this case.

6 CONCLUSIONS

The use of VMS-LES modeling is validated for a collection of bluff body flows in the subcritical regime. Flows around a circular cylinder and a sphere at different Reynolds numbers are considered. Bulk quantities are rather accurately predicted on unstructured grids having resolutions from coarse (sphere case) to moderate. The hybrid model involving VMS-LES also shows a good ability to predict bulk quantities on coarse meshes, even at Reynolds numbers as high as 1-2 millions. We recall that this is rather challenging for a numerical model, since an accurate prediction of bulk quantities requires the boundary-layer and wake evolution to be reasonably well described.

The proposed VMS-LES is still dependent on a coefficient involved in the SGS closure model, which controls the SGS viscosity and must be a-priori assigned. Current investigations focus on a

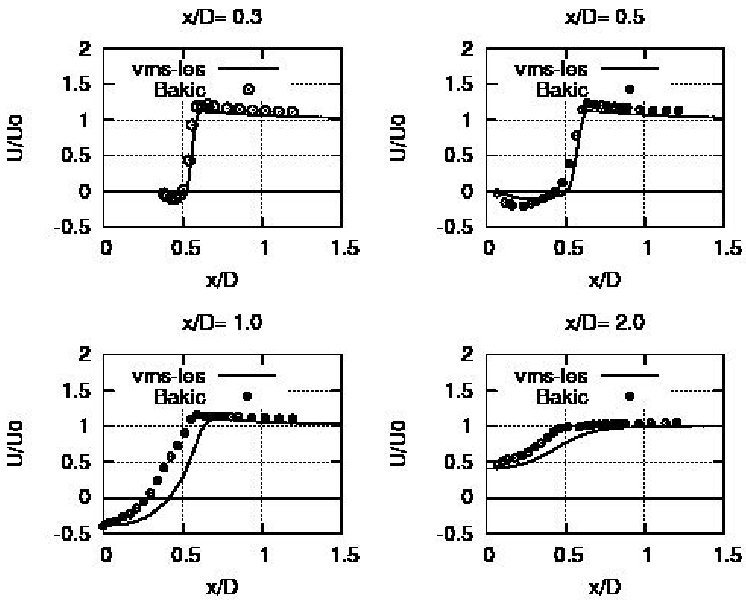

Figure 3: Flow past a sphere at Reynolds 50,000 number: velocity wake and comparison with experiments by Bakic [39]

dynamic version of the SGS viscosity, of low computational cost and combining well to our VMS formulation.

ACKNOWLEDGMENT

This work has been supported by French National Research Agency (ANR) through COSINUS program (project ECINADS n^o ANR-09-COSI-003). HPC resources from GENCI- [CCRT/CINES/IDRIS] (Grant 2009-c2009025067 and 2009-x2009025044) are gratefully acknowledged.

References

[1] S. Camarri, M.V. Salvetti, B. Koobus, and A. Dervieux, Large-eddy simulation of a bluff-body flow on unstructured grids, *Int. J. Num. Meth. Fluids*, 40:1431–1460, 2002.

[2] S. Camarri, M. V. Salvetti, B. Koobus, and A. Dervieux. A low diffusion MUSCL scheme for LES on unstructured grids. *Comp. Fluids*, 33:1101–1129, 2004.

[3] H. Ouvrard, B. Koobus, A. Dervieux, and M.V. Salvetti, Classical and variational multiscale LES of the flow around a circular cylinder on unstructured grids, *Comp. Fluids*, 39:1083–1094, 2010.

[4] T.J.R. Hughes, L. Mazzei, and K.E. Jansen. Large eddy simulation and the variational multiscale method. *Comput. Vis. Sci.*, 3:47–59, 2000.

[5] T.J.R. Hughes and A.A. Oberai and L. Mazzei, Large eddy simulation of turbulent channel flows by the variational multiscale method, *Phys. Fluids*, 13 :1784–1799, 2001.

[6] P. Sagaut, S. Deck, and M. Terracol. *Multiscale and multiresolution approaches in turbulence*. Imperial College Press, London, 2006.

[7] J. Froehlich and D. von Terzi. Hybrid LES/RANS methods for the simulation of turbulent flows. *Prog. Aerosp. Sci.*, 44(5):349–377, 2008.

[8] M.-V. Salvetti, B. Koobus, S. Camarri, A. Dervieux, Simulation of bluff-body flows through a hybrid RANS/VMS-LES model, IUTAM Symposium on Unsteady Separated Flows and their Control, IUTAM Bookseries, 14: 429-440, 2009.

[9] P.L. Roe. Approximate Riemann solvers, parameters, vectors and difference schemes. *J. Comp. Phys.*, 43:357–372, 1981.

[10] H. Guillard and C. Viozat. On the behaviour of upwind schemes in the low Mach number limit. *Computers and Fluids*, 28:63–86, 1999.

[11] U. Goldberg, O. Peroomian, and S. Chakravarthy. A wall-distance-free $k-\varepsilon$ model with enhanced near-wall treatment. *J. Fluids Eng.*, 120:457–462, 1998.

[12] J. Hinze. *Turbulence*. MacGraw-Hill, New York, 1959.

[13] B. Koobus and C. Farhat. A variational multiscale method for the large eddy simulation of compressible turbulent flows on unstructured meshes-application to vortex shedding. *Comput. Methods Appl. Mech. Eng.*, 193:1367–1383, 2004.

[14] J. Smagorinsky. General circulation experiments with the primitive equations. *Monthly Weather Review*, 91(3):99–164, 1963.

[15] F. Nicoud and F. Ducros. Subgrid-scale stress modelling based on the square of the velocity gradient tensor. *Flow Turb. Combustion*, 62(3):183–200, 1999.

[16] E. Achenbach. Distribution of local pressure and skin friction around a circular cylinder in cross-flow up to Re= 5×10^6. *J. Fluid Mech.*, 34(4):625–639, 1968.

[17] M.M. Zdravkovich. *Flow around circular cylinders, Fundamentals, vol.1*. Oxford University press, 1997.

[18] P. Parnaudeau, J. Carlier, D. Heitz and E. Lamballais, Experimental and numerical studies of the flow over a circular cylinder at Reynolds number 3900, *Phys. Fluids*, 20085101, 2008.

[19] A. Kravchenko and P. Moin, Numerical studies of flow over a circular cylinder at $Re_D = 3900$, *Phys. of Fluids*,12:2, 403-417,2000.

[20] J. Lee, N. Park, S. Lee and H. Choi, A dynamical subgrid-scale eddy viscosity model with a global model coefficient, *Phys. Fluids*, 18:12, 2006.

[21] S. Dong and G. E. Karniadakis and A. Ekmekci and D. Rockwell, A Combined DNS-PIV Study of the Turbulent Near Wake, *Journal of Fluid Mechanics*, 569, 185-207, 2006.

[22] J. Ong and L. Wallace, The velocity field of the very near wake of a circular cylinder, *Experiments in Fluids*, vol 20, p 441, 1996.

[23] C. Norberg, Effect of Reynolds number and a low-intensity freestream turbulence on the flow around a circular cylinder, Publ. 87/2. Dept. Applied Thermodynamics and Fluid Mechanics, Chalmers University of Technology, 1987.

[24] C. Norberg, Fluctuating lift on a circular cylinder: review and new measurements, *J. Fluids Struct.*, 17: 57–96, 2003.

[25] R. Gopalkrishnan, Vortex-induced forces on oscillating bluff cylinders, PhD thesis, Department of Ocean Engineering, MIT, Cambridge, MA, USA. 1993.

[26] M. J. Moeller and P. Leehey, Unsteady forces on a cylinder in cross flow at subcritical Reynolds numbers. In ASME Symposium on Flow-induced Vibrations (ed. M. P. Paidoussis, O. M, Griffin and M. Sevik), New Orleans, ASME, New York, vol. 1, pp. 57–71, 1984.

[27] S. Aradag, Unsteady turbulent vortex structure downstream of a three dimensional cylinder, *J. of Thermal Science and Technology* 29(1): 91-98, 2009.

[28] E. Salvatici and M.V. Salvetti, Large-eddy simulations of the flow around a circular cylinder: effects of grid resolution and subgrid scale modeling, *Wind & Structures*, 6(6):419–436, 2003.

[29] H. Lim and S. Lee, Flow Control of Circular Cylinders with Longitudinal Grooved Surfaces, *AIAA Journal*, Vol. 40, No:10, October 2002.

[30] S. Yokuda and R.R. Ramaprian, The dynamics of flow around a cylinder at subcritical reynolds number, *Phys. Fluids A*, 5:3186–3196, 1990.

[31] R.I. Basu, Aerodynamic forces on structures of circular cross-section. part i: Model-scale data obtained under two-dimensional and low-turbulence streams, *J. Wind Eng. Ind. Aerodynamic*, 21:273–294, 1985.

[32] A. Travin, M. Shur, M. Strelets, and P. Spalart. Detached-eddy simulations past a circular cylinder. *Flow Turb. Combustion*, 63:293–313, 1999.

[33] S.-C. Lo, K.A. Hofmann, and J.-F. Dietiker. Numerical investigation of high Reynolds number flows over square and circular cylinder. *J. Thermophys. Heat Trans.*, 19:72–80, 2005.

[34] P. Catalano, Meng Wang, G. Iaccarino, and P. Moin. Numerical simulation of the flow around a circular cylinder at high Reynolds numbers. *Int. J. of Heat and Fluid Flow*, 24:463–469, 2003.

[35] J.W. Schewe. On the forces acting on a circular cylinder in cross flow from subcritical up to transcritical Reynolds numbers. *J. Fluid Mech.*, 133:265–285, 1983.

[36] W.C.L. Shih, C. Wang, D. Coles, and A. Roshko. Experiments on flow past rough circular cylinders at large reynolds numbers. *J. Wind Eng. Indust. Aerodyn.*, 49:351–368, 1993. circular cylinders. *J. Fluid Mech.*, 98(4):673–701, 1980.

[37] O. Guven, C. Farell, and V.C. Patel. Surface-roughness effects on the mean flow past circular cylinders. *J. Fluid Mech.*, 98(4):673–701, 1980.

[38] E. Achenbach Vortex shedding from spheres. *J. Fluid Mech.*, 62(2):209–221, 1974.

[39] V. Bakic *Experimental investigation of turbulent flows around sphere*. PhD thesis, University Harburg-Hamburg, Germany, 2003.